Editors' Suggestion Featured in Physics

# Superconducting-like Heat Current: Effective Cancellation of Current-Dissipation Trade-Off by Quantum Coherence

Hiroyasu Tajima
*Graduate School of Informatics and Engineering, The University of Electro-Communications, 1-5-1 Chofugaoka, Chofu, Tokyo 182-8585, Japan and JST, PRESTO, 4-1-8 Honcho, Kawaguchi, Saitama 332-0012, Japan*

Ken Funo
*Theoretical Physics Laboratory, RIKEN Cluster for Pioneering Reserach, Wako-shi, Saitama 351-0198, Japan*

(Received 22 January 2021; revised 7 July 2021; accepted 13 September 2021; published 4 November 2021)

Quantum coherence is a useful resource for increasing the speed and decreasing the irreversibility of quantum dynamics. Because of this feature, coherence is used to enhance the performance of various quantum information processing devices beyond the limitations set by classical mechanics. However, when we consider thermodynamic processes, such as energy conversion in nanoscale devices, it is still unclear whether coherence provides similar advantages. Here we establish a universal framework, clarifying how coherence affects the speed and irreversibility in thermodynamic processes described by the Lindblad master equation, and give general rules for when coherence enhances or reduces the performance of thermodynamic devices. Our results show that a proper use of coherence enhances the heat current without increasing dissipation; i.e., coherence can reduce friction. In particular, if the amount of coherence is large enough, this friction becomes virtually zero, realizing a superconducting-like "dissipation-less" heat current. Since our framework clarifies a general relation among coherence, energy flow, and dissipation, it can be applied to many branches of science from quantum information theory to biology. As an application to energy science, we construct a quantum heat engine cycle that exceeds the power-efficiency trade-off bound on classical engines and effectively attains the Carnot efficiency with finite power in fast cycles.

DOI: 10.1103/PhysRevLett.127.190604

*Introduction.*—In quantum mechanics, different states can exist simultaneously as a superposition. This feature is the source of many amazing phenomena unique to quantum mechanics, and is expected to provide *quantum advantage* in various tasks. This expectation has proven to be true, at least theoretically, in the field of quantum information theory. In several information processing tasks, such as computation [1,2], communication [3,4], and sensing [5,6], quantum coherence (superposition) can be used to achieve performance beyond the limits imposed by classical mechanics.

On the other hand, there is no clear answer to the question whether coherence has a similar effect in thermodynamic processes. There is still no unified view on even the basic question of whether coherence improves the performance of heat engines [7–14]. This reflects the fact that the relationship between irreversibility and coherence, both of which being the central concepts of thermodynamics and quantum mechanics, is still not clearly understood.

In this Letter, we tackle this problem and establish general rules on how coherence affects the thermodynamic irreversibility in finite-time thermodynamic processes described by the Lindblad master equation, satisfying the detailed balance relation. To achieve this goal, we focus on trade-off relations between thermodynamic irreversibility and the energy flow, a fine refinement of the second law of thermodynamics that has been actively studied in recent years [15–22], and clarify when and to what extent quantum coherence affects the trade-off. Our main results indicate that quantum coherence can enhance the energy flow without increasing irreversibility. In particular, we show that, when the coherence is a large enough, the energy flow obtains an interesting scaling behavior like superconducting electric current. In this case, the energy flow scales as a macroscopic order while keeping dissipation at a constant order, realizing a dissipation-less current.

Our framework provides a general classification on the types of quantum coherence that induce gains or losses in the thermodynamic performance. We find that coherence between energy eigenstates with different energies always induces losses. This is consistent with previous observations that coherence between the ground and excited states that is built up during a heat engine cycle degrades its performance, sometimes termed as the effect of "quantum friction" [8,10]. On the other hand, we find that coherence between degenerate energy eigenstates leads to gains, working as "quantum lubrication."

Since our framework provides a unified understanding among thermodynamic irreversibility, energy flow, and quantum coherence, it has many applications in physics. As an application to energy science, we consider a quantum heat engine that utilizes quantum coherence. We give a general condition about which type of quantum coherence enhances the power and efficiency of heat engines and construct several examples that exceed a universal power-efficiency trade-off relation [18] for classical engines. In particular, we show that the dissipation-less current-driven quantum heat engine approximately attains the Carnot efficiency with finite power in fast cycles. In view of recent proposals on the equivalence between quantum heat engines and natural and artificial light-harvesting systems [23,24], we also discuss possible directions of using our results to understand the role of coherence and its impact on the energy transfer efficiency in light-harvesting systems.

*Setup and results.*—We consider a system connected to multiple heat baths and assume that the time evolution of the reduced density matrix of the system $\rho$ obeys the standard Lindblad master equation [25–29],

$$\frac{\partial \rho}{\partial t} = -\frac{i}{\hbar}[H(t), \rho] + \sum_a \mathcal{D}_a[\rho], \tag{1}$$

where $\mathcal{D}_a[\rho] \coloneqq \sum_\omega \gamma_a(\omega)[L_{a,\omega}\rho L_{a,\omega}^\dagger - \frac{1}{2}\{L_{a,\omega}^\dagger L_{a,\omega}, \rho\}]$ is the dissipator describing the effect of the heat bath labeled by $a$. Here $H(t)$ is the time-dependent Hamiltonian of the system that may have degeneracy, and the Lindblad operator $L_{a,\omega}$ describes a quantum jump between energy eigenstates with energy difference being $\hbar\omega$: $[L_{a,\omega}, H(t)] = \hbar\omega L_{a,\omega}$ [25]. The positive coefficient $\gamma_a(\omega)$ is assumed to satisfy the detailed balance relation $\gamma_a(\omega)/\gamma_a(-\omega) = \exp[\beta_a \hbar\omega]$, where $\beta_a$ is the inverse temperature of the heat bath $a$.

Our purpose is to clarify how coherence affects the trade-off relation between the energy flow and dissipation. For this purpose, we focus on the ratio between the total heat current $J_{\text{tot}} \coloneqq \sum_a |J_a(\rho)|$ and the entropy production rate $\dot{\sigma}$: $J_{\text{tot}}^2/\dot{\sigma}$. Here $J_a(\rho) \coloneqq \text{Tr}[H\mathcal{D}_a[\rho]]$ is the heat current that describes the energy flow from the heat bath $a$ to the system [30]. Also, the entropy production rate is defined as $\dot{\sigma}(\rho) \coloneqq \dot{S}(\rho) - \sum_a \beta_a J_a(\rho) \geq 0$, which is a key quantity that measures dissipation (thermodynamic irreversibility) in stochastic thermodynamics [30–32]. Here, $\dot{S}(\rho) = -\text{Tr}[\partial_t \rho \log \rho]$ is the von Neumann entropy flux of the system [30], and $-\beta_a J_a$ is interpreted as the entropy increase in the heat bath $a$. Therefore, the entropy production quantifies the total amount of entropy that is produced in the entire system, and the second law of thermodynamics is obtained as a direct consequence of the non-negativity of $\dot{\sigma}$. Since the quantities $J_{\text{tot}}$ and $\dot{\sigma}$, respectively, describe the energy flow and dissipation, the current-dissipation ratio $J_{\text{tot}}^2/\dot{\sigma}$ can be interpreted as an indicator for the strength of friction. To support this interpretation, we remark that Joule's law in electric conduction shows that the current-dissipation ratio is inversely proportional to the electric resistance. This ratio also can be used as an indicator for the performance of heat engines because, loosely speaking, large $J_{\text{tot}}$ corresponds to a large output power and small $\dot{\sigma}$ corresponds to a large heat-to-work conversion efficiency.

To evaluate the effect of coherence on the ratio $J_{\text{tot}}^2/\dot{\sigma}$, we denote the energy eigenstates of the Hamiltonian as $|e, j\rangle$, where $e$ is the energy eigenvalue and $j$ is introduced to label degenerate states. We introduce two diagonalized states $\rho_{\text{bd}} \coloneqq \sum_e \Pi_e \rho \Pi_e$ and $\rho_{\text{sd}} \coloneqq \sum_{e,j} \Pi_{e,j} \rho \Pi_{e,j}$, where $\Pi_{e,j} = |e, j\rangle\langle e, j|$ and $\Pi_e = \sum_j \Pi_{e,j}$ is the projection to the eigenspace of $H$ whose eigenvalue is $e$. The subscript "bd" and "sd" are the abbreviations for "block diagonalized" and "strictly diagonalized." In the state $\rho_{\text{bd}}$, coherence between degenerate energy eigenstates is kept, but coherence between different energy eigenspaces is lost. In the state $\rho_{\text{sd}}$, on the other hand, all coherence is lost. Note that if the Hamiltonian is nondegenerate, $\rho_{\text{bd}} = \rho_{\text{sd}}$.

*Result 1. Coherence effects on the current-dissipation ratio*: Now, let us discuss how the quantum coherence affects the current-dissipation ratio $J_{\text{tot}}^2/\dot{\sigma}$. We first show that coherence between different eigenspaces does *not* enhance the current-dissipation ratio [33],

$$\frac{J_{\text{tot}}^2(\rho)}{\dot{\sigma}(\rho)} \leq \frac{J_{\text{tot}}^2(\rho_{\text{bd}})}{\dot{\sigma}(\rho_{\text{bd}})}. \tag{2}$$

According to (2), coherence between different eigenspaces only decreases the ratio $J_{\text{tot}}^2/\dot{\sigma}$. Namely, if the system Hamiltonian has no degeneracy, quantum coherence increases friction and does not improve the performance of heat engines.

We next show that coherence between degenerate energy eigenstates *does* enhance the current-dissipation ratio [33],

$$\frac{J_{\text{tot}}^2(\rho_{\text{sd}})}{\dot{\sigma}(\rho_{\text{sd}})} \leq \frac{A_{\text{cl}}}{2}, \tag{3}$$

$$\frac{J_{\text{tot}}^2(\rho_{\text{bd}})}{\dot{\sigma}(\rho_{\text{bd}})} \leq \frac{A_{\text{cl}} + A_{\text{qm}}}{2}, \tag{4}$$

where the quantities $A_{\text{cl}}$ and $A_{\text{qm}}$ are non-negative real numbers, given by $A_{\text{cl}} \coloneqq \text{Tr}[X\rho_{\text{sd}}]$ and $A_{\text{qm}} \coloneqq \mathcal{C}_X \mathcal{C}_{l_1}(\rho_{\text{bd}})$, with $X \coloneqq \sum_{a,\omega} (\hbar\omega)^2 \gamma_a(\omega) L_{a,\omega}^\dagger L_{a,\omega}$ and $\mathcal{C}_X \coloneqq \max_{e,j,j':j\neq j'} |\langle e, j|X|e, j'\rangle|$. The quantity $\mathcal{C}_{l_1}(\rho_{\text{bd}})$ is the $l_1$-norm of coherence with respect to the eigenstates of the Hamiltonian, which is a well-known coherence measure in the resource theory of coherence [36], defined as the summation of the absolute value of the nondiagonal elements: $\mathcal{C}_{l_1}(\ldots) \coloneqq \sum_{(e,j)\neq(e',j')} |\langle e,j|\ldots|e',j'\rangle|$.

Inequalities (3) and (4) provide general upper bounds on the current-dissipation ratio $J_{\rm tot}^2/\dot{\sigma}$ with and without coherence, respectively. When the state has no coherence, inequality (3) gives a "classical" upper bound $A_{\rm cl}/2$ on the current-dissipation ratio. Namely, heat engines without coherence (i.e., classical heat engines) never exceed this bound. On the other hand, inequality (4) implies that coherence between degenerate eigenstates allows the current-dissipation ratio to exceed its classical limit, up to $A_{\rm qm}/2$. The inequality (4) also shows that this quantum lubrication effect requires nonvanishing $A_{\rm qm}$, which is realized by (i) quantum coherence between degeneracies [to have a nonvanishing $\mathcal{C}_{l_1}(\rho_{\rm bd})$] and (ii) a collective system-bath coupling mechanism such that $L_{a,\omega}$ collectively acts on degenerate energy eigenstates (to have a nonvanishing $\mathcal{C}_X$).

Combining (2) and (4), the upper bound $(A_{\rm cl}+A_{\rm qm})/2$ also applies to a general state $\rho$. Later, we give a quantum heat engine example that demonstrates this quantum lubrication effect and show that the current-dissipation ratio exceeds the classical limitation $A_{\rm cl}/2$ (see Fig. 3).

*Result 2. Dissipation-less heat current*: We further find an interesting scaling behavior in (4) as follows. Suppose that $A_{\rm qm}$ scales as $O(N^2)$, where $2N$ is the number of degeneracy in the system Hamiltonian. Then, the upper bound of the ratio $J_{\rm tot}(\rho)^2/\dot{\sigma}(\rho)$ becomes $O(N^2)$, which allows an $O(1)$ entropy production rate with an $O(N)$ heat current. Therefore, if we can scale up the number of particles and make $N$ macroscopically large, our inequality 4)) implies that large nondiagonal elements and a collective coupling mechanism may produce a macroscopic current without macroscopic dissipation.

The above type of current without dissipation can be realized in a concrete model using the $2N$-state Hamiltonian, given by

$$H = \sum_{j=1}^{N} \hbar\omega_0 |e,j\rangle\langle e,j|, \tag{5}$$

where $|g,j\rangle$ and $|e,j\rangle$ are the $j$th degenerate ground state and excited state, respectively, and $\hbar\omega_0$ is the energy gap (see also Fig. 1). We consider the single bath case (i.e., $a$ takes only a single value) and give the Lindblad jump operators $L_{\omega_0} \coloneqq \sum_{j,j'} |e,j\rangle\langle g,j'|$ and $L_{-\omega_0} \coloneqq L_{\omega_0}^\dagger$, describing collective decays and excitations, to have a nonvanishing $\mathcal{C}_X$. Now, let us prepare an initial state $\rho^+ \coloneqq p_g(0)|g,+\rangle\langle g,+| + p_e(0)|e,+\rangle\langle e,+|$, which has a large amount of coherence $\mathcal{C}_{l_1}(\rho^+) = \mathcal{C}_{l_1}(\rho_{\rm bd}^+) = O(N)$, such that $A_{\rm qm} = O(N^2)$. Here, $p_g(0)/p_e(0) = (1+1/N)e^{\beta\hbar\omega_0}$, where $\beta$ is the inverse temperature of the bath, $|g,+\rangle \coloneqq \sum_j |g,j\rangle/\sqrt{N}$, and $|e,+\rangle \coloneqq \sum_j |e,j\rangle/\sqrt{N}$. As a result, the heat current scales as a macroscopic order while keeping dissipation at a constant order, realizing a dissipation-less current,

$$J_{\rm tot}(\rho^+) = N\hbar\omega_0\gamma(\omega_0)p_e(0) = O(N), \tag{6}$$

$$\dot{\sigma}(\rho^+) = N\log\left(1+\frac{1}{N}\right)\gamma(\omega_0)p_e(0) = O(1). \tag{7}$$

This example demonstrates that when there exists sufficiently large coherence between degeneracies, friction can become vanishingly small via quantum lubrication. We remark that, in the $2N$-state model, the dissipation-less current cannot occur without quantum coherence (see Fig. 1.)

The initially prepared state $\rho^+$ is not the steady state, and therefore the dissipation-less current gradually decreases as the system approaches to the steady state. However, in the Supplemental Material, Sec. II D [33], we construct a dissipation-less current with a steady state by attaching the system to two heat baths.

*Result 3. Finite-time heat engine without dissipation*: By utilizing the dissipation-less current that appears in the $2N$-state model, we can construct a fast heat engine cycle that approximately attains the Carnot efficiency with finite output power. Each step of the heat engine cycle is briefly explained in Fig. 2. For a stationary cycle (i.e., a cycle whose initial and final states are the same), the first law of thermodynamics implies that the extracted work is given by $W = Q_H - Q_C$, where $Q_H = \int_0^{\tau_H} J_H dt > 0$ is the heat absorbed from the hot bath and $Q_C = -\int_0^{\tau_C} J_C dt > 0$ is the heat released to the cold bath. The output power is then defined as the work per unit time: $W/\tau$, where $\tau = \tau_H + \tau_C$. The thermodynamic efficiency is defined as $\eta = W/Q_H$, which quantifies the heat-to-work conversion ratio. Note that $\eta$ is always bounded from above by the Carnot efficiency $\eta_{\rm Car} = 1 - \beta_H/\beta_C$, as a direct consequence of the second law. As we discuss in Supplemental Material,

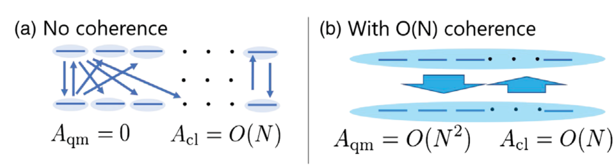


FIG. 1. Schematic diagram of the $2N$-state model. (a) No coherence ($\rho = \rho_{\rm sd}$). In this case, $A_{\rm cl} = O(N)$ and $A_{\rm qm} = 0$ hold for arbitrary $\rho$ (see Supplemental Material, Sec. II B [33]). Therefore, in order to obtain $O(N)$ heat current, dissipation inevitably scales as $O(N)$. (b) With $O(N)$ coherence (e.g., $\rho^+$). In this case, correlated decays and excitations occur and $A_{\rm cl} = O(N)$ and $A_{\rm qm} = O(N^2)$ hold. As a result, an $O(N)$ heat current with a constant-order dissipation is realized.

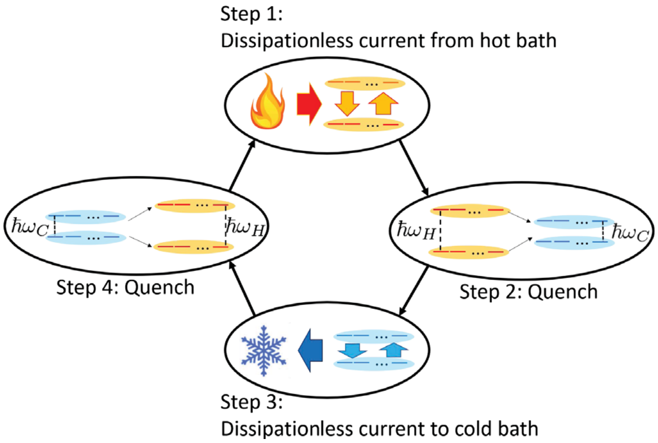


FIG. 2. Schematic diagram of the fast cycle attaining Carnot efficiency with finite power. The cycle consists of four steps. Step 1: the $2N$-state system is connected to the hot bath, absorbing the dissipation-less heat $Q_{\rm H}$ for a time duration $\tau_{\rm H}$. Step 2: the interaction between the system and the hot bath is turned off, and the energy gap of the system is changed from $\hbar\omega_H$ to $\hbar\omega_C$ [37]. Step 3: the system is connected to the cold bath, releasing the dissipation-less heat $Q_{\rm C}$ for a time duration $\tau_{\rm C}$. Step 4: the interaction between the system and the cold bath is turned off, and the energy gap of the system is changed from $\hbar\omega_C$ to $\hbar\omega_H$.

Sec. II C [33], the cycle time of our heat engine can be shorter than the typical relaxation time of the system, and the output power scales as $O(N)$, while the thermodynamic efficiency asymptotically reaches the Carnot efficiency: $\eta = \eta_{\rm Car} - O(1/N)$.

*Result 4. Numerical demonstration of the quantum advantage*: When the number of degeneracy is large, our $2N$-state model approximately achieves the Carnot efficiency with finite power. What if the number of degeneracy is small? Even in this case, our main results indicate interesting properties in the study of quantum heat engines. Here, instead of using the $2N$-state Hamiltonian (5) with $N = 2$, we consider a 2-qubit-state superradiant model that has been experimentally realized with superconducting qubits [38,39] (note that the qualitative behavior of these two models are not different). The Hamiltonian of the system is given by $H = \hbar\omega(\sigma_1^z + \sigma_2^z)$, and the collective jump operator is given by $L = \sigma_1^- + \sigma_2^-$, where $\sigma_i^z$ and $\sigma_i^-$ are the $z$ component of the Pauli operator and the lowering operator for the $i$th qubit. The Lindblad master equation is given by $\partial_t\rho = -(i/\hbar)[H,\rho] + \Gamma_\downarrow[L\rho L^\dagger - (1/2)\{L^\dagger L,\rho\}] + \Gamma_\uparrow[L^\dagger\rho L - (1/2)\{LL^\dagger,\rho\}]$, where $\Gamma_\downarrow = \Gamma_0[1 + \exp(-\beta\hbar\omega)]^{-1}$ and $\Gamma_\uparrow = \Gamma_0[1 + \exp(\beta\hbar\omega)]^{-1}$. When the system is in contact with the hot bath, we set $\omega = \omega_H$ and $\beta = \beta_H$, and the heat current is given by $J_{\rm tot} = J_H$. Note that similar relations hold for the cold bath as well. We use the natural basis of the qubit $\Pi_{e,j} \in \{|g,g\rangle, |g,e\rangle, |e,g\rangle, |e,e\rangle\}$ to define $\rho_{\rm sd}$. We consider the heat engine cycle described above and numerically check the inequalities (3) and (4), plotted in Fig. 3. Then, clearly, the

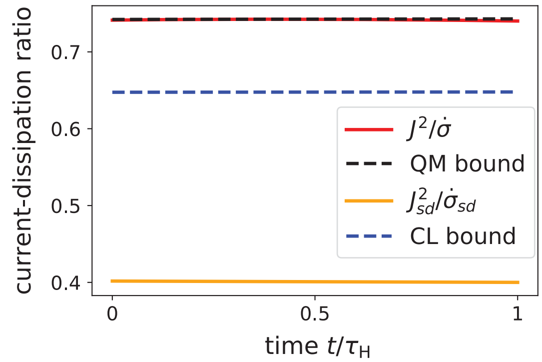


FIG. 3. Numerical check of the current-dissipation trade-off inequalities (3) and (4) as a function of time $t$ during step 1 (interaction with the hot bath) of the 2-qubit heat engine cycle. Red and orange solid curves are the current-dissipation ratio $J_H^2/\dot{\sigma}$ for the states $\rho$ and $\rho_{\rm sd}$, respectively. Black dashed curve is the quantum bound $(A_{\rm cl} + A_{\rm qm})/2$ and the blue dashed curve is the classical bound $A_{\rm cl}/2$. Note that the ratio $J_H^2(\rho)/\dot{\sigma}(\rho)$ exceeds the classical bound, demonstrating the coherence-induced quantum lubrication effect. The parameters are $\omega_H = 1.9$, $\omega_C = 1$, $\beta_H = 1.1$, $\beta_C = 2.1$, $\tau_H = 0.2$, $\Gamma_0 = 1$ (Figs. 3 and 4) and $\tau_C = 0.4$ (Fig. 3).

ratio $J_H(\rho)^2/\dot{\sigma}(\rho)$ exceeds the classical limit $A_{\rm cl}/2$ (note that $\rho = \rho_{\rm bd}$ holds in our example). Finally, from (2)–(4), we obtain the power-efficiency trade-off relation (see Supplemental Material, Sec. IV [33] for details)

$$\frac{W_{\rm cl}/\tau}{\eta_{\rm Car} - \eta_{\rm cl}} \leq c\bar{A}_{\rm cl} \quad \text{and} \quad \frac{W/\tau}{\eta_{\rm Car} - \eta} \leq c(\bar{A}_{\rm cl} + \bar{A}_{\rm qm}), \tag{8}$$

where $c \coloneqq \beta_C\eta_{\rm Car}/[2(2 - \eta_{\rm Car})^2]$ is a constant depending only on $\beta_C$ and $\beta_H$, $\bar{A}_{\rm cl}$ and $\bar{A}_{\rm qm}$ are the time average of $A_{\rm cl}$ and $A_{\rm qm}$ per one engine cycle, and $W_{\rm cl}$ and $\eta_{\rm cl}$ are the work and efficiency for $\rho_{\rm sd}$. The left-hand side of (8) is the ratio between the output power and the deviation of the thermodynamic efficiency from the Carnot efficiency, and thus having a large value of this power-efficiency ratio means that the performance of the heat engine is high. Similar to (4), when there is no coherence, the power-efficiency ratio of the heat engine is bounded by $c\bar{A}_{\rm cl}$. In this sense, $c\bar{A}_{\rm cl}$ is the classical limitation on the performance of heat engines. Meanwhile, when there exists coherence, a quantum heat engine can exceed the classical limitation up to $c\bar{A}_{\rm qm}$. With the 2-qubit superradiant model, we numerically check that the power-efficiency ratio actually exceeds the classical limitation $c\bar{A}_{\rm cl}$ for some parameter range (Fig. 4).

*Applications and discussion.*—Before concluding this Letter, we discuss several applications of our theoretical framework.

*Finite-time Carnot engine*: We gave a heat engine model that approximately attains the Carnot efficiency with finite power. Note that previous studies have utilized nonlinearity

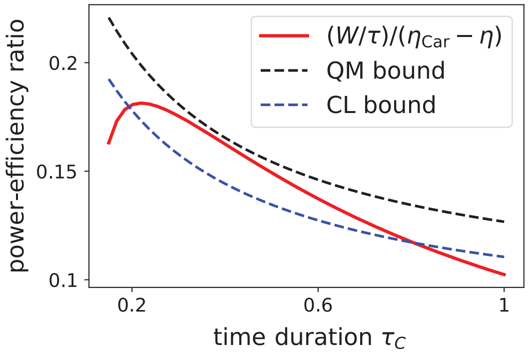


FIG. 4. Numerical calculation of the power-efficiency trade-off relation (8) by varying the time duration $\tau_C$ of the heat engine cycle, step 3. Black dashed curve is the quantum bound $c(\bar{A}_{\rm cl}+\bar{A}_{\rm qm})$ and the blue dashed curve is the classical bound $c\bar{A}_{\rm cl}$. Red solid curve shows the power-efficiency ratio $(W/\tau)\times(\eta_{\rm Car}-\eta)^{-1}$, which exceeds the classical bound for some parameter range.

[40,41], time-reversal symmetry breaking [42,43], non-Markovian effects [44], large heat capacity [45], criticality [46–48], and a large cycle time compared with the relaxation time [49]. On the other hand, our strategy utilizes the dissipation-less current via coherence between degenerate states and a collective system-bath coupling. We note that a collective coupling mechanism requires precise system-bath engineering, and it is challenging for a large system size. However, in view of the experimental progress of realizing superradiance effects [50], we believe that our strategy is meaningful and can be realized with current quantum information technologies.

*Quantitative understanding of the role of coherence in photosynthesis*: An important issue in biology is the role of coherence in photosynthesis [51–56]. Although there are many results reporting the effect of coherence in photosynthetic processes [53–56], there is no unified understandings about how the coherence actually contributes to a high light-harvesting efficiency performance. Since theoretical models are often described by the quantum master equation [53,55], it would be interesting to apply our framework to this problem.

*Thermodynamic meanings of speakable and unspeakable coherence*: In quantum information theory, there are two classes of coherence: speakable coherence and unspeakable coherence [57]. Roughly speaking, speakable coherence refers to the coherence between bases that can be relabeled (e.g., computational basis in a quantum computer). Conversely, unspeakable coherence refers to the coherence between bases that cannot be relabeled (e.g., energy eigenstates with different energy eigenvalues). In our case, the difference between $\rho_{\rm bd}$ and $\rho_{\rm sd}$ reflects the difference between the speakable and unspeakable coherence in $\rho$. Therefore, our results mean that, in the two classes, only the "nonunspeakable" part of the speakable coherence, quantified by $\mathcal{C}_{l_1}(\rho_{\rm bd})$, contributes to the performance enhancement.

In this Letter, we gave a unified understanding of how quantum coherence affects the thermodynamic irreversibility for open quantum systems obeying the Lindblad master equation satisfying the detailed balance relation, through the current-dissipation ratio. Our results can be summarized in three basic rules as follows: 1. Quantum friction: coherence between different energy eigenspaces always reduces the ratio. 2. Quantum lubrication: when the system collectively interacts with the bath, coherence between degenerate states can be used to increases the ratio. 3. Dissipation-less current: if there is enough coherence between degenerate states, the heat current can become macroscopic order, while dissipation remains at constant order. From the observations, we have demonstrated the quantum advantage in the performance of heat engines enhancement in the 2-qubit system example and have constructed a heat engine model that effectively attains the Carnot efficiency with finite power.

Our dissipation-less current induced by coherence resembles the superconducting current without energy dissipation, induced by large off-diagonal components. In addition, unlike the discussions of the vanishing local resistance in a mesoscopic (quantum phase-coherent) contact [58], our $2N$-state model produces a large current between two heat baths, while the (global) entropy production effectively vanishes. We expect that our findings will further contribute to the understandings and design of low-dissipative energy transporting mechanisms in energy science, biology, and condensed matter physics.

Our results completely cover the cases described by the Lindblad master equation, satisfying the detailed balance relation. On the other hand, for other cases, the general relationship between coherence and irreversibility is still unknown. We would like to close this Letter by pointing out that this problem is still an open question.

We thank H. Hayakawa and Y. Hino for discussions and helpful comments. We acknowledge support from the JSPS KAKENHI [Grants No. JP19K14610 (H. T.) and No. JP18J00454 (K. F.)], JST PRESTO (H. T., Grant No. JPMJPR2014), JST MOONSHOT (H. T. Grant No. JPMJMS2061), and the Foundational Questions Institute Fund, a donor advised fund of Silicon Valley Community Foundation (K. F., Grant No. FQXi-IAF19-06).

[1] D. Deutsch and R. Jozsa, Rapid solution of problems by quantum computation, Proc. R. Soc. A **439**, 553 (1992).

[2] P. W. Shor, Algorithms for quantum computation: Discrete logarithms and factoring, in *Proceedings of the 35th Annual Symposium on Foundations of Computer Science* (IEEE Computer Society Press, Los Alamitos, California, 1994),

pp. 124–134, https://dx.doi.org/10.1109/SFCS.1994.365700.

[3] C. H. Bennett and S. J. Wiesner, Communication via One- and Two-Particle Operators on Einstein-Podolsky-Rosen States, Phys. Rev. Lett. **69**, 2881 (1992).

[4] C. H. Bennett and G. Brassard, Quantum cryptography: Public key distribution and coin tossing, Theor. Comput. Sci. **560**, 7 (2014).

[5] V. Giovannetti, S. Lloyd, and L. Maccone, Quantum-enhanced measurements: Beating the standard quantum limit, Science **306**, 1330 (2004).

[6] V. Giovannetti, S. Lloyd, and L. Maccone, Quantum Metrology, Phys. Rev. Lett. **96**, 010401 (2006).

[7] R. Uzdin, A. Levy, and R. Kosloff, Equivalence of Quantum Heat Machines, and Quantum-Thermodynamic Signatures, Phys. Rev. X **5**, 031044 (2015).

[8] K. Brandner, M. Bauer, and U. Seifert, Universal Coherence-Induced Power Losses of Quantum Heat Engines in Linear Response, Phys. Rev. Lett. **119**, 170602 (2017).

[9] H. P. Goswami and U. Harbola, Thermodynamics of quantum heat engines, Phys. Rev. A **88**, 013842 (2013).

[10] A. del Campo, A. Chenu, S. Deng, and H. Wu, Friction-free quantum machines, in *Thermodynamics in the Quantum Regime*, edited by F. Binder, L. Correa, C. Gogolin, J. Anders, and G. Adesso, Fundamental Theories of Physics Vol. 195 (Springer, Cham, 2018), https://doi.org/10.1007/978-3-319-99046-0_5.

[11] C. L. Latune, I. Sinayskiy, and F. Petruccione, Energetic and entropic effects of bath-induced coherences, Phys. Rev. A **99**, 052105 (2019).

[12] C. L. Latune, I. Sinayskiy, and F. Petruccione, Thermodynamics from indistinguishability: Mitigating and amplifying the effects of the bath, Phys. Rev. Research **1**, 033192 (2019).

[13] J. Klatzow, J. N. Becker, P. M. Ledingham, C. Weinzetl, K. T. Kaczmarek, D. J. Saunders, J. Nunn, I. A. Walmsley, R. Uzdin, and E. Poem, Experimental Demonstration of Quantum Effects in the Operation of Microscopic Heat Engines, Phys. Rev. Lett. **122**, 110601 (2019).

[14] C. L. Latune, I. Sinayskiy, and F. Petruccione, Negative contributions to entropy production induced by quantum coherences, Phys. Rev. A **102**, 042220 (2020).

[15] A. C. Barato and U. Seifert, Thermodynamic Uncertainty Relation for Biomolecular Processes, Phys. Rev. Lett. **114**, 158101 (2015).

[16] J. M. Horowitz and T. R. Gingrich, Thermodynamic uncertainty relations constrain non-equilibrium fluctuations, Nat. Phys. **16**, 15 (2020).

[17] U. Seifert, From stochastic thermodynamics to thermodynamic inference, Annu. Rev. Condens. Matter Phys. **10**, 171 (2019).

[18] N. Shiraishi, K. Saito, and H. Tasaki, Universal Trade-off Relation between Power and Efficiency for Heat Engines, Phys. Rev. Lett. **117**, 190601 (2016).

[19] N. Shiraishi and H. Tajima, Efficiency versus speed in quantum heat engines: Rigorous constraint from Lieb-Robinson bound, Phys. Rev. E **96**, 022138 (2017).

[20] N. Shiraishi and K. Saito, Fundamental relation between entropy production and heat current, J. Stat. Phys. **174**, 433 (2019).

[21] S. Ito and A. Dechant, Stochastic Time-Evolution, Information Geometry and the Cramer-Rao Bound, Phys. Rev. X **10**, 021056 (2020).

[22] A. Dechant, Multidimensional thermodynamic uncertainty relations, J. Phys. A **52**, 035001 (2019).

[23] K. E. Dorfman, D. V. Voronine, S. Mukamel, and M. O. Scully, Photosynthetic reaction center as a quantum heat engine, Proc. Natl. Acad. Sci. U.S.A. **110**, 2746 (2013).

[24] C. Creatore, M. A. Parker, S. Emmott, and A. W. Chin, Efficient Biologically Inspired Photocell Enhanced by Delocalized Quantum States, Phys. Rev. Lett. **111**, 253601 (2013).

[25] H.-P. Breuer and F. Petruccione, *The Theory of Open Quantum Systems* (Oxford University Press, New York, 2002).

[26] For the conditions of the realization of time-dependent Hamiltonians in Lindblad master equations satisfying the detailed balance relation, see [27–29].

[27] T. Albash, S. Boixo, D. A Lidar, and P. Zanardi, Quantum adiabatic Markovian master equations, New J. Phys. **14**, 123016 (2012).

[28] M. Yamaguchi, T. Yuge, and T. Ogawa, Markovian quantum master equation beyond adiabatic regime, Phys. Rev. E **95**, 012136 (2017).

[29] R. Dann, A. Levy, and R. Kosloff, Time-dependent Markovian quantum master equation, Phys. Rev. A **98**, 052129 (2018).

[30] K. Funo, M. Ueda, and T. Sagawa, Quantum fluctuation theorems, in *Thermodynamics in the Quantum Regime*, edited by F. Binder, L. Correa, C. Gogolin, J. Anders, and G. Adesso, Fundamental Theories of Physics Vol. 195 (Springer, Cham, 2018), https://doi.org/10.1007/978-3-319-99046-0_10.

[31] K. Sekimoto, *Stochastic Energetics*, Lecture Notes in Physics Vol. 799 (Springer-Verlag, Berlin, Heidelberg, 2010).

[32] U. Seifert, Stochastic thermodynamics, fluctuation theorems and molecular machines, Rep. Prog. Phys. **75**, 126001 (2012).

[33] See Supplemental Material at http://link.aps.org/supplemental/10.1103/PhysRevLett.127.190604 for additional results, detailed proofs, and extended discussions, which includes Refs. [34,35]. In Sec. I, we give derivations of inequalities (2)–(4).

[34] M. A. Nielsen and I. L. Chuang, *Quantum Information and Quantum Computation* (Cambridge University Press, Cambridge, England, 2000).

[35] K. Funo, N. Shiraishi, and K. Saito, Speed limit for open quantum systems, New J. Phys. **21**, 013006 (2019).

[36] T. Baumgratz, M. Cramer, and M. B. Plenio, Quantifying Coherence, Phys. Rev. Lett. **113**, 140401 (2014).

[37] We note that step 2 (and also step 4) can be completed instantaneously by quenching the Hamiltonian. Since the Hamiltonian before and after the quench commute with each other, dissipation does not occur during those processes.

[38] A. F. van Loo, A. Fedorov, K. Lalumière, B. C. Sanders, A. Blais, and A. Wallraff, Photon-mediated interactions between distant artificial atoms, Science **342**, 1494 (2013).

[39] X. Gu, A. F. Kockum, A. Miranowicz, Y.-X. Liu, and F. Nori, Microwave photonics with superconducting quantum circuits, Phys. Rep. **718–719**, 1 (2017).

[40] M. Ponmurugan, Attainability of maximum work and the reversible efficiency from minimally nonlinear irreversible heat engines, arXiv:1604.01912.

[41] J. Koning and J. O. Indekeu, Engines with ideal efficiency and nonzero power for sublinear transport laws, Eur. Phys. J. B **89**, 248 (2016).

[42] G. Benenti, K. Saito, and G. Casati, Thermodynamic Bounds on Efficiency for Systems with Broken Time-Reversal Symmetry, Phys. Rev. Lett. **106**, 230602 (2011).

[43] M. Mintchev, L. Santoni, and P. Sorba, Thermoelectric efficiency of critical quantum junctions, arXiv:1310.2392.

[44] A. E. Allahverdyan, K. V. Hovhannisyan, A. V. Melkikh, and S. G. Gevorkian, Carnot Cycle at Finite Power: Attainability of Maximal Efficiency, Phys. Rev. Lett. **111**, 050601 (2013).

[45] P. Abiuso and M. Perarnau-Llobet, Optimal Cycles for Low-Dissipation Heat Engines, Phys. Rev. Lett. **124**, 110606 (2020).

[46] M. Polettini, G. Verley, and M. Esposito, Efficiency Statistics at All Times: Carnot Limit at Finite Power, Phys. Rev. Lett. **114**, 050601 (2015).

[47] M. Campisi and R. Fazio, The power of a critical heat engine, Nat. Commun. **7**, 11895 (2016).

[48] C. V. Johnson, Exact model of the power-to-efficiency trade-off while approaching the Carnot limit, Phys. Rev. D **98**, 026008 (2018).

[49] V. Holubec and A. Ryabov, Cycling Tames Power Fluctuations near Optimum Efficiency, Phys. Rev. Lett. **121**, 120601 (2018).

[50] A. Angerer, K. Streltsov, T. Astner, S. Putz, H. Sumiya, S. Onoda, J. Isoya, W. J. Munro, K. Nemoto, J. Schmiedmayer, and J. Majer, Superradiant emission from colour centres in diamond, Nat. Phys. **14**, 1168 (2018).

[51] Y.-C. Cheng and G. R. Fleming, Dynamics of light harvesting in photosynthesis, Annu. Rev. Phys. Chem. **60**, 241 (2009).

[52] G. S. Engel, T. R. Calhoun, E. L. Read, T.-K. Ahn, T. Mančal, Y.-C. Cheng, R. E. Blankenship, and G. R. Fleming, Evidence for wavelike energy transfer through quantum coherence in photosynthetic systems, Nature (London) **446**, 782 (2007).

[53] M. Mohseni, P. Rebentrost, S. Lloyd, and A. Aspuru-Guzik, Environment-assisted quantum walks in photosynthetic energy transfer, J. Chem. Phys. **129**, 174106 (2008).

[54] A. Ishizaki and G. R. Fleming, Theoretical examination of quantum coherence in a photosynthetic system at physiological temperature, Proc. Natl. Acad. Sci. U.S.A. **106**, 17255 (2009).

[55] P. Rebentrost, M. Mohseni, and A. Aspuru-Guzik, Role of quantum coherence and environmental fluctuations in chromophoric energy transport, J. Phys. Chem. B **113**, 9942 (2009).

[56] E. Romero, R. Augulis, V. I. Novoderezhkin, M. Ferretti, J. Thieme, D. Zigmantas, and R. van Grondelle, Quantum coherence in photosynthesis for efficient solar-energy conversion, Nat. Phys. **10**, 676 (2014).

[57] I. Marvian and R. W. Spekkens, How to quantify coherence: Distinguishing speakable and unspeakable notions, Phys. Rev. A **94**, 052324 (2016).

[58] Y. Imry and R. Landauer, Conductance viewed as transmission, Rev. Mod. Phys. **71**, S306 (1999).